

Protein antifouling and fouling-release in perfluoropolyether surfaces

Elena Molena^a, Caterina Credi^a, Carmela De Marco^a, Marinella Levi^a, Stefano Turri^{a,*}, Giovanni Simeone^b

^a Dipartimento di Chimica, Materiali e Ingegneria Chimica "Giulio Natta", Politecnico di Milano, Piazza Leonardo da Vinci 32, 20133 Milan, Italy

^b Solvay Specialty Polymers spa, R&D Center, Viale Lombardia 20, Bollate, MI, Italy

Article history:

Received 13 March 2014

Received in revised form 24 April 2014

Accepted 30 April 2014

Available online 9 May 2014

1. Introduction

Anti-fouling materials have attracted a significant interest, especially as marine coatings and in biotechnology. In the former case they are used to prevent biofouling adhesion on ship hulls [1], thus reducing hydrodynamic drag and fuel consumption, while in biochemistry and biotechnology anti-fouling surfaces allow for the design and realization of protein resistant devices and components [2]. Anti-fouling and fouling-release are two different concepts. The former means preventing the adhesion of fouling organisms or proteins in static conditions, while the latter involves the possibility of removing them dynamically by the hydrodynamic forces exerted through a fluid flow.

A well-known protein anti-fouling polymer largely applied in biomedical and biological research is poly(ethylene glycol) (PEG) [2,3]. Ostuni et al. [4] studied a variety of self-assembled monolayers (SAMs) with different functional groups to explain the protein binding resistance of PEG. They showed that the interaction of surface with water and PEG charge neutrality are fundamental issues for anti-fouling properties.

On the other hand, atoxic fouling-release industrial coatings have been proposed as sustainable products for applications in marine environments [5]. To avoid the use of toxic chemicals [6]

like tin salts, atoxic release coatings based on silicones and fluoropolymers have been developed. In particular, perfluoropolyether (PFPE) functional oligomers, largely used as building blocks [7,8,9] for high performance protective coatings and water/oil repellant surface treatments, are promising for this application [10,11].

The increasing diffusion of microfluidic devices for biomedical uses has led toward the development of fouling-release materials also for their fabrication [12,13]. Actually, UV curable perfluoropolyether-dimethacrylates (PFPE-DMA) have been used for device microfabrication [13] and more recently amphiphilic structures containing both hydrophilic and hydrophobic moieties have been proposed as potential fouling-release coatings. De Simone et al. [14] described also blends of photocurable perfluoropolyether-dimethacrylate/polyethylene glycol-methacrylate polymeric (PFPE/PEG blend), and studied the effect of the PEG chain molecular weight on fouling-release properties against spores. Other works in the literature have tested the effectiveness of other perfluoropolyether polymers as protein-adhesion resistant substrate [15]. In contrast to the available information concerning biofouling release properties of perfluoropolyether coatings, very little is known about the mechanism of molecular interaction of perfluoropolyether surfaces and proteins.

The main topic of our work is to study the behavior of perfluoropolyether polymers as protein adhesion resistant substrates, which can be applied in the realization of microfluidic

* Corresponding author. Tel.: +39 223993252.
E-mail address: stefano.turri@polimi.it (S. Turri).

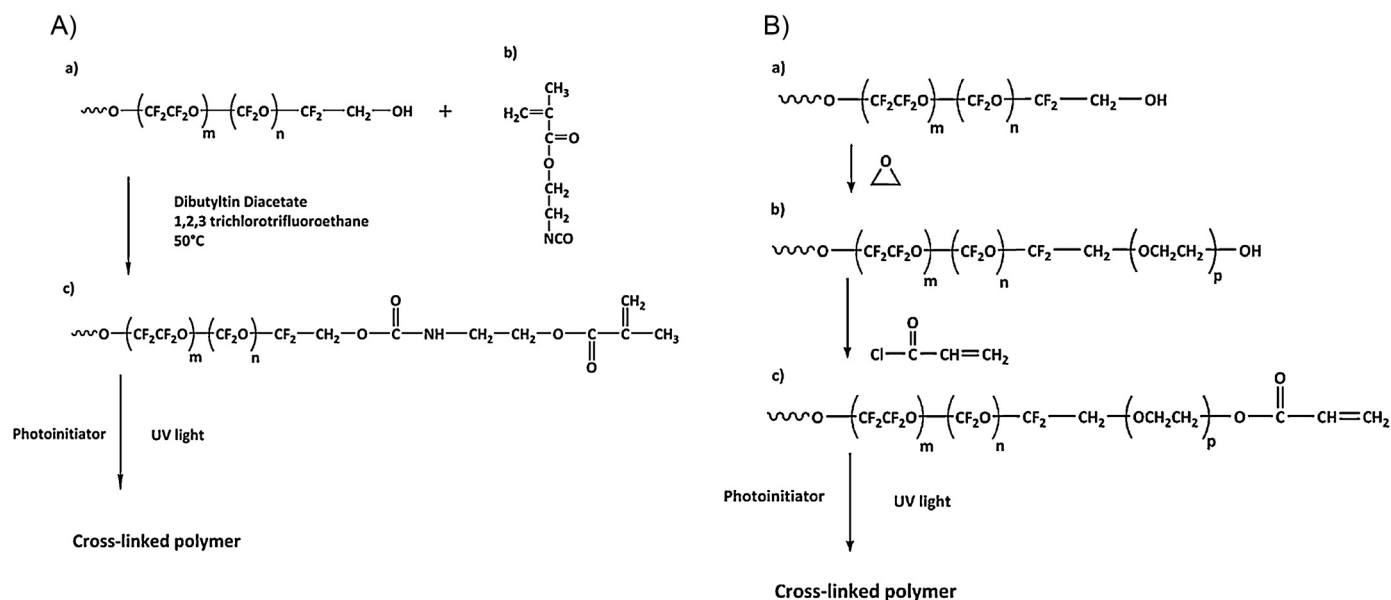


Fig. 1. (A) Perfluoropolyether dimethacrylates (c) obtained from the reaction of a perfluoropolyether macrodiol (a) with an isocyanate ethyl methacrylate (b); (B) perfluoropolyether poly(ethylene glycol) diacrylates obtained from a perfluoropolyether diol (a) by the sequential addition of a poly(ethylene glycol) chain (b) and finally of acrylic end chain groups (c).

biomedical devices. Different UV curable perfluoropolyether polymers, copolymers and blends are described, fully characterized, and their protein antifouling and fouling-release behavior is investigated. The main structural parameters [16,17] affecting their functional behavior are highlighted, giving useful information for the design and selection of high performance, protein resistant PFPE surfaces.

2. Experimental

2.1. Perfluoropolyether materials

One PFPE urethane dimethacrylate oligomer (commercial name: Fluorolink™ MD700) was provided by Solvay Specialty Polymers (Bollate, Italy), and will be indicated as PFPE-DMA 2000 in the following. The main properties are $M_n = 1980$ g/mol; density = 1.66 g/ml. A higher molecular weight version of the PFPE urethane dimethacrylate was synthesized in our laboratory starting from a perfluoropolyether macrodiol (Fluorolink™ D4000, Solvay Specialty Polymers) with $M_n = 4000$ g/mol, following the experimental procedure reported by Priola et al. [18] using isocyanatoethylmethacrylate (IEM, Alfa Aesar) for the functionalization reaction. PFPE-PEG-DAs were kindly provided by Solvay Specialty Polymers; here the PFPE macromer is chain-extended by two PEG segments and endcapped by acrylic groups through ester bond. In particular, two PFPE-PEG-DA grades that differ for the number of repeating PEG units were characterized in terms of surface and anti-fouling/fouling-release properties. The former PFPE-PEG-DA sample has a $M_n = 2030$ g/mol and is characterized by an average of 4.6 ethylene glycol (EG) repeating units in the backbone; the latter with $M_n = 2206$ g/mol, is made of 8 EG repeating units. The chemical structures of PFPE oligomers are shown in Fig. 1. PFPE surfaces were prepared by adding 4% (w/w) of photoinitiator (Darocur 1173, Ciba) with the exception of PFPE-DMA 4000 that was prepared by adding 1% of 2,2-dimethoxy-2-diphenylacetophenone (Sigma-Aldrich). All surfaces were exposed to UV light for crosslinking. UV irradiation was made with a bromograph (MF 1030, Nuova Delta Elettronica, Italy)

under vacuum. The bromograph contained 4 UV-A lamps of 15 W each, with an emitted power density of 4 mW/cm².

2.2. Contact angle measurement

Samples for contact angle measurements were prepared by spin coating (750 rpm, 1 min) (ws400 6npp lite, Laurell Technologies Corp.) on well cleaned glass panels. The contact angle measurements were performed using an optical video contact angle system (OCA-15-plus, Dataphysics, Germany). The static contact angle was measured using the sessile drop method with dedicated software (SCA 2.0) determining the contact angle based on the Young-Laplace fitting. A 1 μl droplet of water (Chromasolv water for HPLC, Sigma-Aldrich) was dispensed on the sample using the electronic syringe unit of the instrument equipped with a 500 μl Hamilton syringe. The measurement was repeated several times on different areas on the substrate. The same procedure was followed using diiodomethane (Sigma-Aldrich), because at least two liquids are necessary to compute surface tension. Surface tension was obtained by applying the harmonic mean equation [19] to find both the dispersive and the polar components. Dynamic measurements were done by increasing the drop volume in the wetting process (advancing contact angle) and then decreasing it in the de-wetting phase (receding contact angle). The syringe needle remained in the drop during the whole process. In the first wetting phase a 3 μl drop was created on the solid surface and then slowly increased in volume. In the second phase the surface was de-wetted and the drop size reduced. The whole cycle was repeated 5 times at 1 $\mu\text{l/s}$, with a delay time of 1 s between each cycle. Advancing and receding angles are computed by the tangent at the three-phase contact line.

2.3. Dynamic mechanical analysis

Samples for dynamic-mechanical analysis were prepared by casting 0.5–1.0 g of oligomer in a rounded cap having diameter of 24 mm. A silicone rubber layer was placed on the top, and the sample was exposed to UV-light for 10 min. After complete cross-linking PFPE films were punched to obtain disks having

Table 1
Static contact angle values against water.

Material	Average values [°]
PFPE-DMA 2000	110 ± 1
PFPE-DMA 4000	113 ± 1
PFPE-PEG 4.6-DA	103 ± 1
PFPE-PEG 8-DA	107 ± 1

diameter of 15 mm. By controlling the amount of prepolymer poured in the cap it was possible to obtain films with controlled thickness of 600–700 μm . The dynamic-mechanical test was performed using a Mettler Toledo DMA/SDTA 861 dynamic mechanical analyzer in shear sandwich mode. All samples were tested at 0.1 Hz with $T = 23^\circ\text{C}$ and 70°C , and G' values were obtained as a function of oscillation amplitude. G' values in the linear viscoelastic range were extrapolated to obtain Young modulus values.

2.4. Evaluation of anti-fouling and fouling-release properties

The assessment of anti-fouling and fouling-release properties of polymer surfaces was performed using fluorescein isothiocyanate bovine serum albumin (BSA-FITC) (Sigma-Aldrich) as the test protein. Different materials were tested to benchmark the performances of PFPE photopolymers. Polymethylmethacrylate (PMMA, PerspexTM by Lucite) and polydimethylsiloxane [20] (PDMS, SylgardTM 184 by Dow Corning) are known to absorb proteins, while polyethylene glycol [21] (PEG) is a typical anti-fouling material. In particular, a PEG based photopolymer [22] was included in the experiments, and will be indicated as PEG-MA in the following. Also a photocurable PFPE/PEG blend was taken from the literature [23], and tested to compare its non-fouling properties. The PFPE/PEG blend was a mixture of polyethylene glycol monomethacrylate having molecular weight of 450 g/mol and PFPE-DMA 2000 in weight ratio 10:90. The blend was made photocurable by adding 4% of Darocur 1173 and finally the solution was stirred for 30 min.

In conclusion, the complete set of test materials was: PMMA, PDMS, PEG-MA, PFPE/PEG blend, PFPE-DMA 2000, PFPE-DMA 4000, PFPE-PEG 4.6-DA and PFPE-PEG 8-DA.

As far as anti-fouling static tests are concerned, 3 mg of BSA-FITC were dissolved in 30 ml of distilled water to prepare a 0.01% (w/v) solution. Three drops of solution, having a volume of 200 μl each, were poured on the substrates. The samples were then taken for 60 min on a hot plate at 37°C . Finally, every sample was rinsed in abundant distilled water twice, and let dry for 25 min on a hot plate at 37°C .

Fouling-release dynamic tests were performed using a microfluidic pump (Syringe Pump 11 Plus, Harvard Apparatus) and a home-made microfluidic channel system. Micrometric channels were fabricated bonding a flat surface made of the chosen substrate material (PFPE, PDMS, PMMA or PEG) with a PDMS channel obtained by replica of an SU-8 channel. Channel dimensions were $500\ \mu\text{m} \times 200\ \mu\text{m}$. The albumin solution was then pumped into

Table 2
Surface tension values measured by the Wu approach that enables to find both dispersive and polar components.

Material	SFT polar [mN/m]	SFT dispersive [mN/m]	SFT total [mN/m]
PFPE-DMA 2000	3.2 ± 0.4	12.5 ± 0.4	15.8 ± 0.3
PFPE-DMA 4000	3.5 ± 0.4	12.1 ± 0.7	15.6 ± 0.4
PFPE-PEG 4.6-DA	13.6 ± 0.4	6.2 ± 0.6	19.8 ± 0.5
PFPE-PEG 8-DA	13.6 ± 0.7	4.8 ± 0.5	18.4 ± 0.4

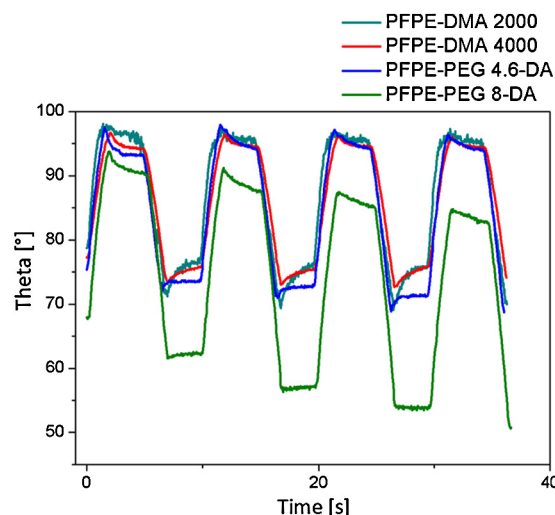


Fig. 2. Dynamic contact angle measurements showing a thermodynamic hysteresis for all perfluoropolyether polymers and a significant kinetic hysteresis for PFPE-PEG 8-DA.

the micro-fluidic system at the chosen flow rate. Finally, samples were rinsed by fluxing distilled water at 100 $\mu\text{l}/\text{min}$ in the same channel.

Observation by a fluorescence microscope (Olympus Ix70 inverted microscope) allows for the estimation of the protein adsorption on the substrates. Image elaboration was performed by Image JTM software which enabled us to obtain the graphical representation of the tonal distribution (image histogram) of digital fluorescent images for a quantitative comparison. The standard deviation was calculated averaging the mean tonal values of three different images for each sample material.

3. Results and discussion

The release properties of polymeric materials like silicones and fluoropolymers relies on their physico-chemical properties; in particular surface tension and elastic modulus seem to play an extremely important role. The relationship between surface free energy and bioadhesion has been deeply investigated in the literature. R.E. Baier was the first to study the role of surface tension

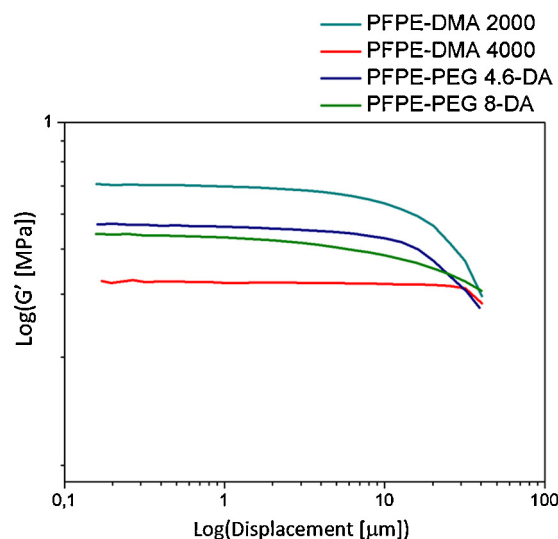


Fig. 3. Dynamic shear moduli vs oscillation amplitude measured by Dynamic Mechanical Analysis performed at 70°C and 0.1 Hz.

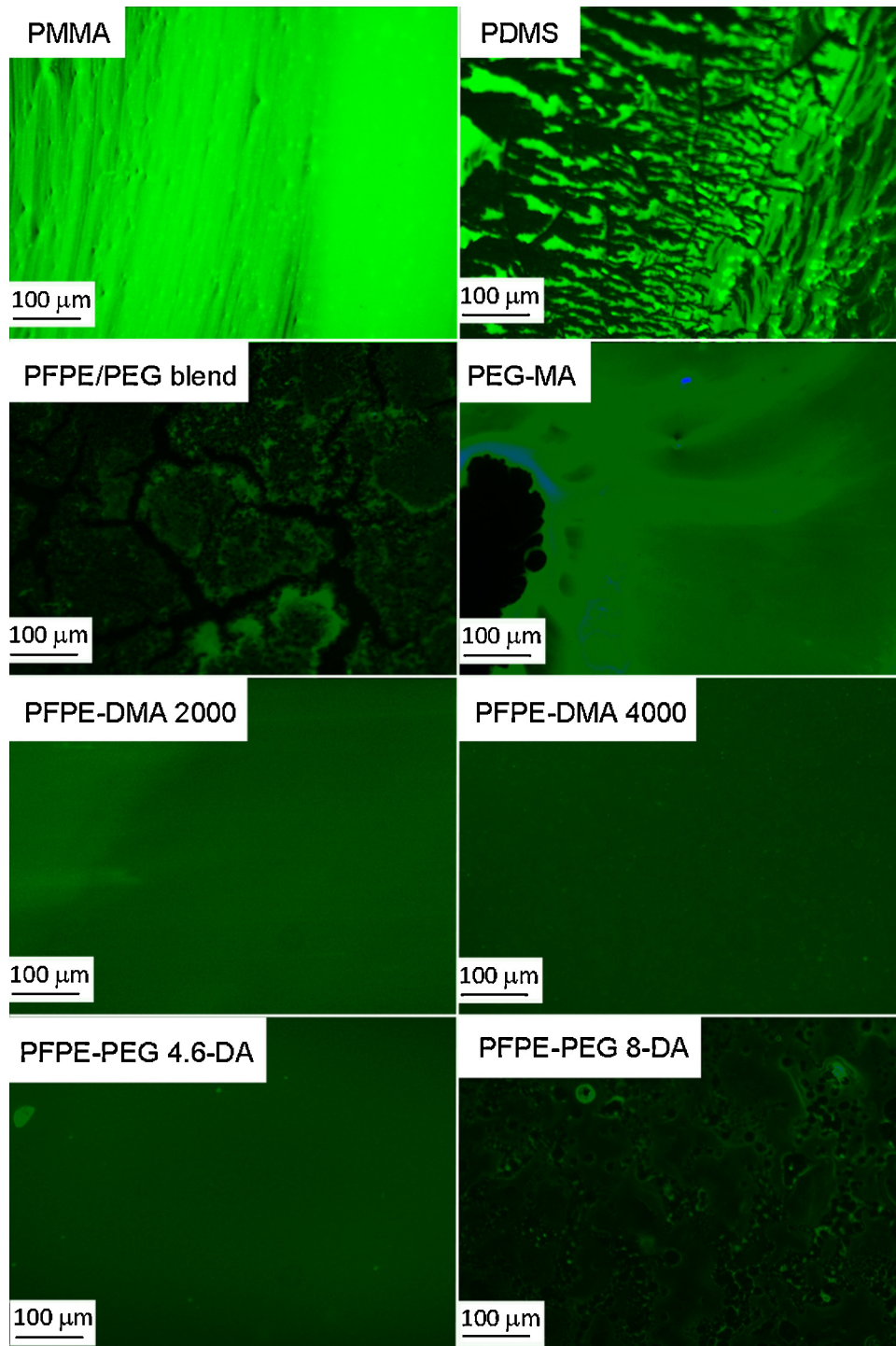


Fig. 4. Static test samples observed by fluorescence microscopy (magnification 10 \times , exposure time 200 ms, the substrate area observed is 650 μm \times 500 μm).

on the adhesion of blood proteins and platelets [24], but similar considerations were then applied to the field of marine biofouling prevention [25]. These studies revealed that protein/fouling adhesion decreases linearly with surface tension up to 25 mN/m, which is the value of PDMS; a further diminishment of surface tension would not be beneficial. Baier proposed that a critical surface tension value between 20 and 30 mJ/m² is ideal in preventing bioadhesion [26]. However, more recent studies suggested that surface tension must be considered keeping in mind also the elastic modulus of the material. A more comprehensive approach is to study fouling adhesion against $(E\gamma)^{1/2}$ to study the combined effect

of both elastic modulus and surface tension [27,28]. Considering both factors, PFPE polymers are certainly promising fouling-release materials, having both low elastic modulus and low surface tension. A low surface tension is crucial for the initial attachment of proteins, while the elastic modulus of the substrate mainly affects the fouling release properties, since it induces the joint formed between the substrate and the protein to fail by peel rather than by shear. Finally, also the coating thickness plays a role, since less force is needed to remove a fouling layer from a thicker coating [16,17]. The joint between proteins and the coating can be studied in terms of fracture mechanics, from which the dependence

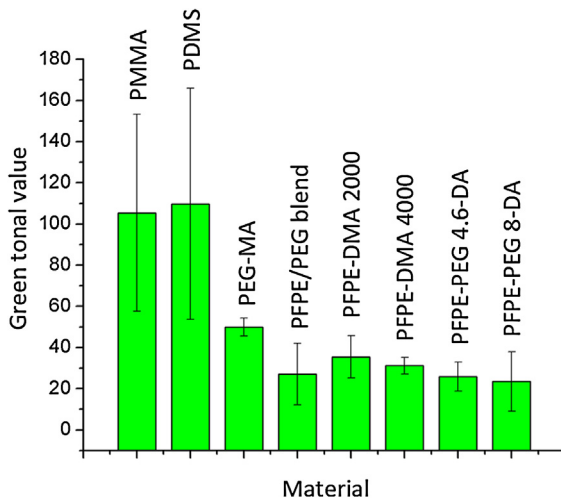


Fig. 5. Mean tonal value for each sample tested in static conditions. PDMS and PMMA give the brightest images while PFPE-PEG 8-DA and PFPE/PEG blend the darkest.

of fouling-release performance on $(E\gamma)^{1/2}$ is derived. The approach stems from the well-known Griffith theory that shows how fracture of solids depends not only on surface energy but also on geometry and the elastic properties of the materials. Considering the case of a thin film of thickness ' t ' and Young's modulus ' E ' sandwiched between an infinite rigid plane and a disk of diameter ' $2a$ ', we can obtain an expression for the peel force, shown in Eq. (1).

$$P^2 = \frac{2\pi^2 K a^4 \gamma}{t} \quad (1)$$

where ' P ' is the peel force necessary to the joint failure, ' a ' is the contact radius, ' t ' is the coating thickness and ' K ' is the bulk modulus, that is related to the elastic modulus through the Poisson coefficient ' ν ' as shown in Eq. (2).

$$E = 3K(1 - 2\nu) \quad (2)$$

Combining Eqs. (1) and (2), it is evident the connection between fouling-release properties and $(E\gamma)^{1/2}$. However, it must be noted that other parameters such as surface reconstruction [29] and surface roughness may play a role in the assessment of fouling-release properties.

3.1. Polymer molecular structures

All polymers studied in this paper are composed of three main parts: a central perfluoropolyether backbone, two more polar lateral segments and terminal photocurable moieties. Hence, the molecular structure can be schematized as [30] $G-R_h$ -PFPE- R_h - G , where G is the photoreactive group, R_h is the polar moiety and finally PFPE refers to the main perfluoropolyether chain. For PFPE-DMA the photoreactive G unity is represented by a methacrylic group, while R_h refers to the lateral polar urethane group as represented in Fig. 1A. PFPE-PEG-DAs instead are composed of acrylic photoreactive groups (G) and lateral polar poly(ethylene glycol) segments (R_h), as represented in Fig. 1B.

3.2. Surface tension

Surface tension values were obtained from static contact angle measurements by applying the Wu approach. Tables 1 and 2 report values about static contact angle and surface tension components respectively.

The results of static contact angle measurements show that all PFPE-based surfaces are hydrophobic, with a water contact angle well above 90° . PFPE-PEG-DA polymers show a lower contact angle due to the presence of the polar poly (ethylene glycol) chain.

Considering the London and the Debye–Keesom theories [19], the Wu approach is able to discriminate between polar and dispersive components of surface tension. As far as PFPE-DMA are concerned the dispersive component is predominantly associated to the fluorocarbon moiety, while the polar one is related to the urethane groups. Given that the fraction of urethane groups is much smaller than to the fluorocarbon chain, we can explain why the dispersive component is predominant. On the other hand, PFPE-PEG-DAs show a higher surface energy and the predominance of the polar component associated to the hydrophilic poly (ethylene glycol) chain in the molecular backbone.

3.3. Contact angle hysteresis

From the difference between advancing and receding contact angles, the contact angle hysteresis was found. As shown in Fig. 2 all PFPE-based materials showed a clear hysteresis due to the presence of chemically heterogeneous domains [31].

Kinetic contact angle hysteresis, i.e. the change of hysteresis value in time, is the indication of molecular rearrangements of functional groups at the solid–liquid interface [32]. As shown in Fig. 2 receding and advancing contact angles are quite constant over time for PFPE-DMA, revealing a pure thermodynamic behavior. On the contrary a kinetic behavior was detected on PFPE-PEG-DAs, associated to the surface rearrangement of the polar poly (ethylene glycol) chain stimulated by the contact with water. Given that the polar component is higher for PFPE-PEG-DAs, a higher surface group rearrangement is expected with respect to PFPE-DMA, as confirmed by our experimental results. The higher molecular weight PFPE-PEG-DA shows the highest value of hysteresis likely due to the higher length of the PEG blocks and the lower density of crosslinking of the polymeric network. We can also notice that for PFPE-PEG-DAs the molecular weight strongly influences surface properties while both perfluoropolyether dimethacrylates show a similar surface behavior; the change in molecular weight of the lateral segments R_h has a stronger impact on surface properties than the molecular weight increase of the main perfluoropolyether chain.

3.4. Dynamic-mechanical properties

The results of dynamic mechanical analysis performed on PFPE-DMA and PFPE-PEG-DAs are reported in Fig. 3, concerning a strain sweep at $+65^\circ\text{C}$ therefore well within the rubbery plateau of the material. Moduli values were measured on two samples of the same material and then averaged.

The higher shear modulus of PFPE-DMA 2000 with respect to PFPE-DMA 4000 can be attributed to its higher cross-link density that is the consequence of a shorter perfluoropolyether chain between methacrylic end chain groups. Similar considerations can be applied to explain the higher shear modulus of the PFPE-PEG 4.6-DA with respect to the higher molecular weight PFPE-PEG-DA. From Fig. 3 we can also notice the wide gap between shear moduli of the PFPE-DMA compared that of PFPE-PEG-DAs. Doubling the length of the perfluoropolyether main chain has a stronger influence on mechanical properties than the molecular weight increase of lateral poly (ethylene glycol) segments. We can conclude that the change in molecular weight of lateral segments mainly affects surface properties while the molecular weight increase of the

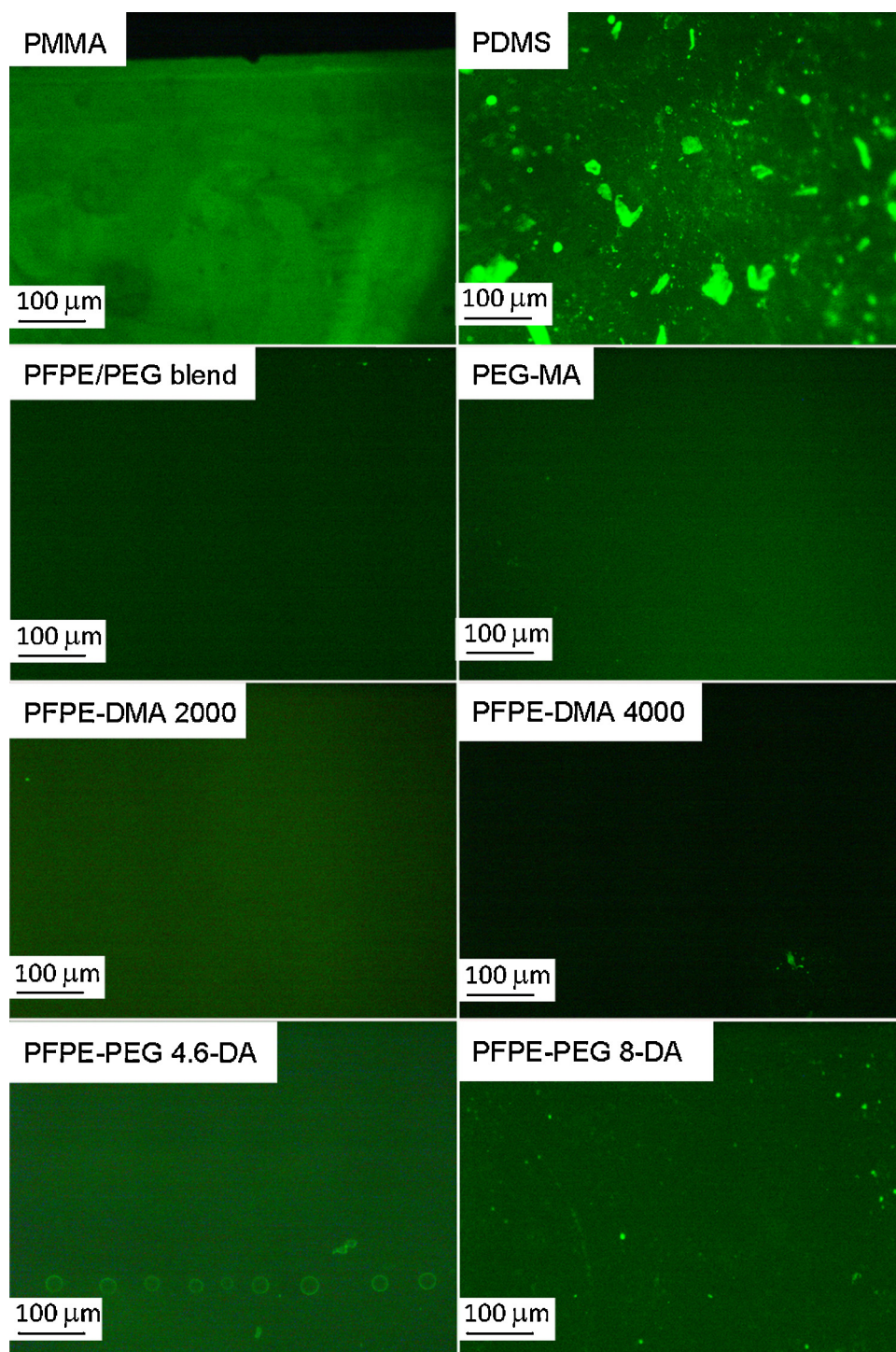


Fig. 6. Dynamic test results. Exposure time: 400 ms.

perfluoropolyether backbone has a stronger effect on mechanical properties.

3.5. Anti-fouling and fouling-release properties

Static anti-fouling properties and dynamic fouling-release properties were evaluated first from a qualitative point of view comparing fluorescent images, then in a more quantitative way after image analysis and elaboration. Figs. 4 and 5 report respectively the qualitative and quantitative evaluation of static anti-fouling behavior.

As expected, the most intense fluorescence signal was observed on PMMA and PDMS surfaces that show an appreciable difference in signal intensity with respect to other samples. On the contrary, all PFPE-based polymers show fluorescence signals comparable to PEG-MA, a well-established anti-fouling substrate. A quantitative comparative analysis allows for the rationalization of the results shown in Fig. 4.

Image brightness is an indication of BSA-FITC adherence on the substrate. The results confirm that BSA can efficiently adhere to PDMS and PMMA while all PFPE based materials show antifouling properties similar to PEG-MA. On the other hand, a residual

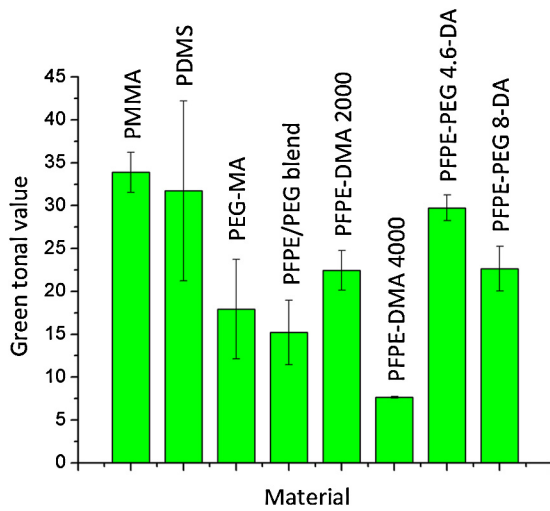


Fig. 7. Mean tonal value for each sample tested in static conditions. PDMS and PMMA give the brightest images while PFPE-DMA 4000 seems to be the best candidates for fluidic applications.

fluorescence is always present in all surfaces. As can be noted from Fig. 5, standard deviation is low on PFPE-based surfaces meaning that appreciable differences between surfaces of the same material are not detectable. Opposite considerations can be done for PDMS and PMMA that show a relevant variability from sample to sample.

In Figs. 6 and 7 the results of fouling-release tests are shown.

As a general observation, all the substrates show a significantly lower fluorescence with respect to results of static tests. PDMS and PMMA both in static and dynamic conditions allow the adhesion of BSA-FITC. PFPE-DMA 2000 with both PFPE-PEG 4.6-DA, PFPE-PEG 8-DA and PFPE-PEG blend show similar brightness, comparable to PEG-MA. The best candidate for microfluidic applications seems to be PFPE-DMA 4000, which shows the lowest fluorescent signal compared to other materials. This means that BSA-FITC was easily detached by hydrodynamic forces in our test conditions.

From quantitative analysis, PFPE-DMA 4000 was identified as the most promising material that can be thus classified as an efficient fouling-release substrate. Another aspect that is worth mentioning is the good reproducibility of PFPE-DMA 4000 experimental behavior as demonstrated by the very low standard deviation.

3.6. Surface and mechanical properties influence on fouling release properties

As explained at the beginning of this paragraph, fouling-release properties are correlated to both surface tension and elastic modulus. A linear dependence of fouling-release performance on $(E\gamma)^{1/2}$ was predicted [17]. A similar analysis was performed in this work to verify the applicability of such considerations to our study, focusing on the results of perfluoropolyether-based materials that showed the best anti-fouling and fouling-release results. The fouling-release performance of perfluoropolyether polymers represented by the mean tonal value was plotted against $(E\gamma)^{1/2}$ as shown in Fig. 8a.

In Fig. 8a, although a general trend is not clear, we can still identify some subgroups. Increasing $(E\gamma)^{1/2}$, a worsening in the fouling-release performance can be noticed going from PFPE-DMA 4000 to PFPE/PEG blend and to PFPE-DMA 2000. The same can be noticed for PFPE-PEG-DAs; PFPE-PEG 8-DA, having a lower $(E\gamma)^{1/2}$, shows a better behavior with respect to PFPE-PEG 4.6-DA. The deviation of PFPE-PEG-DAs from the first subgroup may be attributed to other phenomena. Surface rearrangements revealed from dynamic contact angle measurements may play a role favoring the exposure of hydrophilic groups on the surface. The loss of the fluorine atoms sheath on the surface may lead to increased protein binding. More interesting conclusions for perfluoropolyether materials can be drawn considering separately the contribution of polar and dispersive components, that implicitly means to take into account the effect of dynamic contact angle hysteresis. As shown in Fig. 8b a general trend for all PFPE-based materials can be identified, so that a lower value of $(E\gamma_{\text{polar}})^{1/2}$ corresponds to a better performance in terms of fouling-release properties. It is important to highlight that mechanical properties seem to give a significant contribution to fouling-release properties at least within a well-defined class of polymeric substrates. Despite having comparable surface energies, PFPE-DMA 2000 and 4000 show a different fouling-release performance and a similar reasoning can be applied to PFPE-PEG-DAs. Thus, it would seem that in this case the most significant contribution comes from the stiffness of the surface layer. Since we have noticed that the perfluoropolyether backbone mainly influences mechanical properties, we can conclude that the molecular weight of the main perfluoropolyether chain may significantly affect the fouling-release performance. However, if the same data fitting is applied to the whole set of experimental data including PMMA, PEG-MA and PDMS, the correlation is poor and no clear trend seems to exist (data not shown).

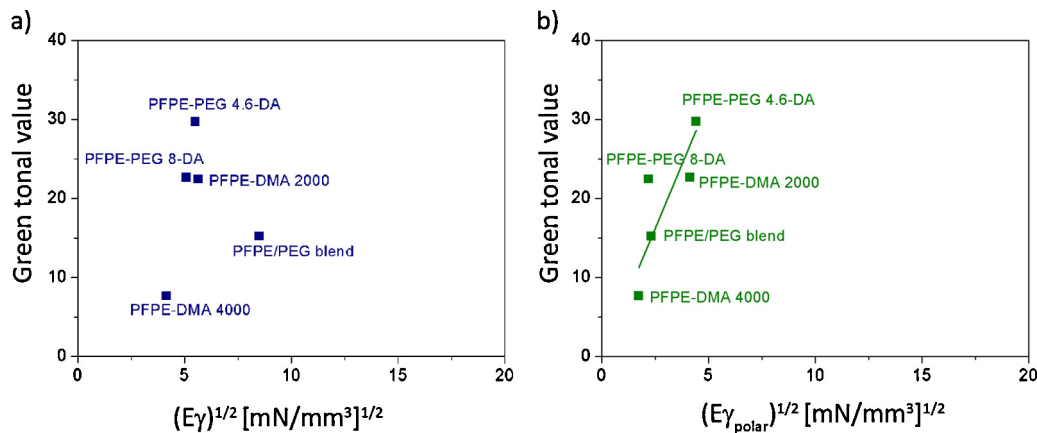


Fig. 8. Fouling-release performance dependence on a parameter depending on both surface tension and mechanical properties (a) considering the total component of surface tension; (b) considering only the polar component of surface tension. In the second case a better correlation was found.

4. Conclusions

The anti-fouling/fouling-release behavior against protein adhesion of several perfluoropolyethers was deeply investigated with the aim to find a suitable material for protein adhesion resistant biomedical devices and for microfluidic devices applied to biochemistry. Moreover, different kinds of perfluoropolyethers were characterized in terms of surface and mechanical properties to find a way to predict the fouling-release performance from other material properties. Our study revealed a linear dependence of the fouling-release performance on a parameter containing both surface energy and elastic modulus. The perfluoropolyether dimethacrylate with higher molecular weight showed the best fouling-release performance due to the low surface energy but, most important, to the low elastic modulus. Finally, it has to be stressed that such tests were done with only one kind of protein. A deeper analysis involving the test of these materials with a wider spectrum of proteins should be performed to investigate general behaviors. In conclusion, our studies have shown that all perfluoropolyethers have good anti-fouling/fouling-release properties but in particular low surface energy, high molecular weight of the PFPE chain between cross-link points and the absence of surface group rearrangement (kinetic hysteresis) seem to be important requirements for the design of anti-fouling/fouling-release materials. Copolymerization of PFPEs with PEG to give linear segmented structures did not show any significant improvement, suggesting that extremely low surface tension materials perform better than amphiphilics especially in dynamic behavior. Alternative strategies for the design and realization of higher performance amphiphilic PFPE-PEG surfaces may actually involve the copolymerization of bifunctional perfluoropolyethers and monofunctional graft polyethylene glycol chains through the use of polyfunctional macromers like for example polyisocyanates or triazines.

Appendix A. Supplementary data

Supplementary data associated with this article can be found, in the online version.

References

- [1] L.D. Chambers, K.R. Stokes, F.C. Walsh, R.J.K. Wood, Modern approaches to marine antifouling coatings, *Surf. Coat. Technol.* 201 (2006) 3642–3652.
- [2] A. Bajpai, Blood protein adsorption onto a polymeric biomaterial of polyethylene glycol and poly[(2-hydroxyethyl methacrylate)-co-acrylonitrile] and evaluation of in vitro blood compatibility, *Polym. Int.* 54 (2005) 304–315.
- [3] P. Kim, D.H. Kim, B. Kim, S.K. Choi, S.H. Lee, A. Khademhosseini, et al., Fabrication of nanostructures of polyethylene glycol for applications to protein adsorption and cell adhesion, *Nanotechnology* 16 (2005) 2420–2426.
- [4] E. Ostuni, B. Grzybowski, M. Mrksich, C. Roberts, G.M. Whitesides, Adsorption of proteins to hydrophobic sites on mixed self-assembled monolayers, *Langmuir* 19 (2003) 1861–1872.
- [5] D.M. Yebra, S. Kiil, K. Dam-Johansen, Antifouling technology – past, present and future steps towards efficient and environmentally friendly antifouling coatings, *Prog. Org. Coat.* 50 (2004) 75–104.
- [6] R.F. Brady Jr., No more tin: what now for fouling control? *J. Prot. Coat. Linings* 17 (2000).
- [7] T. Trombetta, P. Iengo, S. Turri, Fluorinated segmented polyurethane anionomers for water–oil repellent surface treatments of cellulosic substrates, *J. Appl. Polym. Sci.* 98 (2005) 1364–1372.
- [8] S. Turri, S. Radice, R. Canteri, G. Speranza, M. Anderle, Surface study of perfluoropolyether–urethane cross-linked polymers, *Surf. Interface Anal.* 29 (2000) 873–886.
- [9] G. Simeone, S. Turri, M. Scicchitano, C. Tonelli, Fundamental properties of fluoropolyether-based resins and related coatings, *Die Angew. Makromol. Chem.* 236 (1996) 111–127.
- [10] Z. Hu, J.A. Finlay, L. Chen, D.E. Betts, M.A. Hillmyer, M.E. Callow, et al., Photochemically cross-linked perfluoropolyether-based elastomers: synthesis, physical characterization, and biofouling evaluation, *Macromolecules* 42 (2009) 6999–7007.
- [11] J.C. Yarbrough, J.P. Rolland, J.M. DeSimone, M.E. Callow, J.A. Finlay, J.A. Callow, Contact angle analysis, surface dynamics, and biofouling characteristics of cross-linkable, random perfluoropolyether-based graft terpolymers, *Macromolecules* 39 (2006) 2521–2528.
- [12] C. De Marco, S. Girardo, E. Mele, R. Cingolani, D. Pisignano, Ultraviolet-based bonding for perfluoropolyether low aspect-ratio microchannels and hybrid devices, *Lab Chip* 8 (2008) 1394–1397.
- [13] J.P. Rolland, R.M. Van Dam, D.A. Schorzman, S.R. Quake, J.M. Desimone, V. Uni, et al., Solvent-resistant photocurable “Liquid Teflon” for microfluidic device fabrication, *J. Am. Chem. Soc.* (2004) 2322–2323.
- [14] Y. Wang, L.M. Pitet, J.A. Finlay, L.H. Brewer, G. Cone, D.E. Betts, et al., Investigation of the role of hydrophilic chain length in amphiphilic perfluoropolyether/poly(ethylene glycol) networks: towards high-performance antifouling coatings, *Biofouling* 27 (2011) 1139–1150.
- [15] S. Kwon, H. Kim, J.-W. Ha, S.-Y. Lee, Prevention of protein and polymeric nanoparticles adsorption using perfluoropolyether, *J. Ind. Eng. Chem.* 17 (2011) 259–263.
- [16] K. Kendall, The adhesion and surface energy of elastic solids, *J. Phys. D: Appl. Phys.* 4 (2002) 1186–1195.
- [17] R.F. Brady, A fracture mechanical analysis of fouling release from nontoxic antifouling coatings, *Prog. Org. Coat.* 43 (2001) 188–192.
- [18] A. Priola, R. Bongiovanni, G. Malucelli, A. Pollicino, C. Tonelli, G. Simeone, UV-curable systems containing perfluoropolyether structures: synthesis and characterisation, *Macromol. Chem. Phys.* 198 (1997) 1893–1907.
- [19] S. Wu, Polar and nonpolar interactions in adhesion, *J. Adhes.* 5 (1973) 39–55.
- [20] K.Y. Chumbimuni-Torres, R.E. Coronado, A.M. Mfuh, C. Castro-Guerrero, M.F. Silva, G.R. Negrete, et al., Adsorption of proteins to thin-films of PDMS and its effect on the adhesion of human endothelial cells, *RSC Adv.* 1 (2011) 706.
- [21] S. Sharma, R.W. Johnson, T.A. Desai, XPS and AFM analysis of antifouling PEG interfaces for microfabricated silicon biosensors, *Biosens. Bioelectron.* 20 (2004) 227–239.
- [22] S. Turri, M. Levi, E. Emilriti, R. Suriano, R. Bongiovanni, Direct photopolymerisation of peg-methacrylate oligomers for an easy prototyping of microfluidic structures, *Macromol. Chem. Phys.* 211 (2010) 879–887.
- [23] Y. Wang, D.E. Betts, J.A. Finlay, L. Brewer, M.E. Callow, J.A. Callow, et al., Photocurable amphiphilic perfluoropolyether/poly(ethylene glycol) networks for fouling-release coatings, *Macromolecules* 44 (2011) 878–885.
- [24] R.E. Baier, Human platelet spreading on substrata of known surface chemistry, *Bull. N. Y. Acad. Med.* 48 (1972) 257.
- [25] R.F. Brady, Properties which influence marine fouling resistance in polymers containing silicon and fluorine, *Prog. Org. Coat.* 35 (1999) 31–35.
- [26] R.E. Baier, V.A. Depalma, D.W. Goupil, E. Cohen, Human platelet spreading on substrata of known surface chemistry, *J. Biomed. Mater. Res.* 19 (1985) 1157–1167.
- [27] C.M. Magin, S.P. Cooper, A.B. Brennan, Non-toxic antifouling strategies, *Mater. Today* 13 (2010) 36–44.
- [28] Z. Hu, Novel Perfluoropolyethers as Fouling-Release Coatings, University of North Carolina, 2009.
- [29] C.S. Gudipati, J.A. Finlay, J.A. Callow, M.E. Callow, K.L. Wooley, The antifouling and fouling-release performance of hyperbranched fluoropolymer (HBFP)-poly(ethylene glycol) (PEG) composite coatings evaluated by adsorption of biomacromolecules and the green fouling alga *Ulva*, *Langmuir* 21 (2005) 3044–3053.
- [30] R. Bongiovanni, A. Medici, A. Zompatori, S. Garavaglia, C. Tonelli, Perfluoropolyether polymers by UV curing: design, synthesis and characterization, *Polym. Int.* 61 (2012) 65–73.
- [31] C.W. Extrand, Contact angles hysteresis on surfaces with chemically heterogeneous islands, *Langmuir* 19 (2003) 3793–3796.
- [32] C. Chan, Polymer Surface Modification and Characterization, Carl Hanser, GmbH & Co., 1993.